Predictive geospatial model for arsenic accumulation in Holocene aquifers based on interactions of oxbow-lake biogeochemistry and alluvial geomorphology

Devanita Ghosh [a,b,*], Marinus Eric Donselaar [c,d]

[a] Sanitary Engineering Section, Water Management Department, Delft University of Technology, the Netherlands
[b] Laboratory of Biogeochem-mystery, Centre for Earth Sciences, Indian Institute of Science, Bangalore, India
[c] Department of Geoscience and Engineering, Delft Univ. of Technology, P.O. Box 5048, 2600 GA Delft, the Netherlands
[d] Department of Earth and Environmental Sciences, Division of Geology, KU Leuven, Celestijnenlaan 200E, B-3001 Leuven, Belgium

HIGHLIGHTS

- Oxbow lakes are sinks to natural and anthropogenic organic C & N.
- Elevated fluxes of organics induce methanogenesis & microbial reductive dissolution of As.
- Tracers (microbial and organic-biomarkers) suggest sewage contamination of aquifers.
- Sandy point bars confined by clay plugs are effective arsenic traps.
- Poro-perm anisotropy in alluvial deposits rules the spatial distribution of As.

GRAPHICAL ABSTRACT
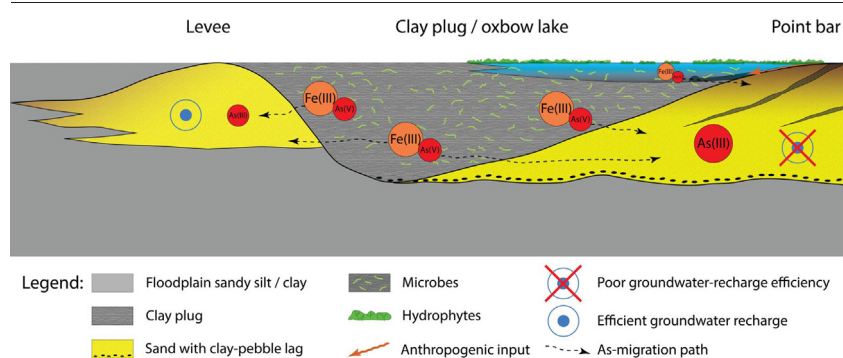
ARTICLE INFO

ABSTRACT

The identification of arsenic-contamination hotspots in alluvial aquifers is a global-scale challenge. The collection and inventory of arsenic concentration datasets in the shallow-aquifer domain of affected alluvial basins is a tedious and slow process, given the magnitude of the problem. Recent research demonstrates that oxbow-lake biogeochemistry in alluvial plains, mobilization of geogenic arsenic, and accumulation in geomorphologically well-defined areas are interacting processes that determine arsenic-contamination locations. This awareness provides a tool to identify potential arsenic-hotspots based on geomorphological similarity, and thus contribute to a more robust and targeted arsenic mitigation approach. In the present study, a conceptual predictive geospatial model is proposed for the accumulation of dissolved arsenic as a function of interaction of oxbow-lake biogeochemistry and alluvial geomorphology. A comprehensive sampling campaign in and around two oxbow lakes in the Jamuna River Basin, West Bengal (India) provided water samples of the oxbow-lake water column for analysis of dissolved organic matter (DOM) and microbial communities, and groundwater samples from tube wells in point bars and fluvial levees bordering the oxbow lakes for analysis of the geospatial distribution of arsenic in the aquifer. Results show that abundant natural and anthropogenic (faecal-derived) recalcitrant organic matter like coprostanols and sterols in clay-plug sediment favours microbial (heterotrophs, enteric pathogens) metabolism and arsenic mobilization. Arsenic concentrations in the study area are highest (averaging 505 μg/L) in point-bar aquifers geomorphologically enclosed by partially sediment-filled oxbow lakes, and much lower (averaging 121 μg/L) in wells of levee sands beyond the oxbow-lake confinement. The differences reflect variations in groundwater recharge efficiency as result of the porosity and permeability anisotropy in the alluvial geomorphological elements, where arsenic-rich groundwater is trapped in point-bars enclosed by oxbow-lake

---

* Corresponding author at: Sanitary Engineering Section, Water Management Department, Delft University of Technology, the Netherlands.
E-mail address: D.Ghosh@tudelft.nl (D. Ghosh).

clays and, by contrast, levee ridges are not confined on all sides, resulting in a more efficient aquifer flushing and decrease of arsenic concentrations.

1. Introduction

Forty years have passed since the global threat of arsenic toxicity from groundwater contamination was first realized (Das et al., 1994; Acharyya et al., 2000; BGS and DPHE, 2001; Smedley and Kinniburgh, 2002; Ahmed et al., 2004; Ravenscroft et al., 2009; Podgorski and Berg, 2020). Ever since, research into the occurrence of toxic natural arsenic levels above the recommended upper limit of 10 μg/L (World Health Organization (WHO), 2011) in food, drinking and irrigation water from groundwater sources has greatly advanced our knowledge of all aspects of the arsenic issue, from its provenance to transport modes and deposition in sedimentary basins, uptake by humans and its severe health impact for many millions of people around the world (Guha Mazumder, 2003; Saha, 2003; Chikkanna et al., 2019; Kavil et al., 2020). The wide range of natural-arsenic studies deals with: (1) Identification of the provenance of natural arsenic in orogenic mountain belts (Göd and Zemann, 1999; Horton et al., 2001; Campbell et al., 2004; Mukherjee et al., 2014, 2019; Tapia et al., 2019, among others), (2) The accumulation of geogenic arsenic in Holocene floodbasins as solid-state arsenic iron-oxyhydroxides, arseno-pyrites, biotite (Bhattacharya et al., 2006; Bundschuh et al., 2004; Berg et al., 2007; Huang et al., 2011; Ramos et al., 2014; Kumar et al., 2021a; among others), (3) The role of microbial metabolism processes in the mobilization of arsenic from its solid state and subsequent accumulation in alluvial-plain aquifers (Nickson et al., 1998, 2000; Acharyya et al., 2000; Acharyya and Shah, 2007; Seddique et al., 2008; Lawson et al., 2013; Sahu and Saha, 2015; Donselaar et al., 2017; Ghosh and Bhadury, 2018; Ghosh et al., 2021), (4) The health risks of arsenic uptake by food, water consumption and irrigation (Islam et al., 2000; Zhao et al., 2010; Rahman et al., 2018; Roychowdhury et al., 2018; Kavil et al., 2020; Zhao and Wang, 2020; Kumar et al., 2021b; Mondal et al., 2021), and (5) the development of arsenic mitigation strategies based on the improved knowledge of the arsenic contamination problem (Hoque et al., 2006: Howard et al., 2006; Jakariya et al., 2007; Chakraborti et al., 2013; Hossain et al., 2015, 2017; Sathe and Mahanta, 2019).

Despite the enormous extent of aquifer contamination in Holocene alluvial basins around the world, and the unpredictably large geospatial variability in arsenic concentrations, recent research advances show that the interaction of two factors is pivotal for arsenic-hotspot occurrence in the shallow aquifer domain (Donselaar et al., 2017; Ghosh et al., 2021; Kumar et al., 2021c; Raju, 2022; Singh et al., 2022): (a) the key role of microbial metabolism in the reductive dissolution process of As-bearing Fe(II) oxy-hydroxides in anoxic oxbow lakes rich in labile organic matter, and (b) the stratigraphical and geomorphological heterogeneity of the alluvial landscape prone in arsenic toxicity. Studies with focus on the abundance of arsenic concentration in the Holocene lithostratigraphy and the drop of concentrations in underlying Pleistocene stratigraphy have yielded a generalized perspective of stratigraphic control on arsenic distribution in shallow aquifers of alluvial floodbasins (e.g., Bhattacharya et al., 2006; Berg et al., 2007; Aziz et al., 2008; Guo et al., 2008; Van Geen et al., 2008, 2013; Weinman et al., 2008; Hoque et al., 2009, 2014; McArthur et al., 2011; Robinson et al., 2011; Postma et al., 2012, 2016; Sahu and Saha, 2015; Stopelli et al., 2020; Wallis et al., 2020; Kazmierczak et al., 2022). Mukherjee et al. (2010), Donselaar et al. (2017), Cao et al. (2018), Trung et al. (2020), Das and Mondal (2021), Ghosh et al. (2021), and Kumar et al. (2021a) have taken the concept of lithostratigraphic control one step further by relating porosity and permeability anisotropy in genetically-related, juxtaposed (1) clayey floodplain and oxbow-lake, and (2) sandy point-bar and fluvial levee geomorphological units, to geospatial

differences in aquifer flushing efficiency and, consequently, to the accumulation of arsenic in poorly-flushed pockets (Michael and Voss, 2008).

The dynamic process of biologically refractive (humic-like) organic molecules plays a major role in aquifers in aqueous complexation (Sharma et al., 2010; Liu et al., 2011) and electron shuttling. The awareness of the interacting processes of oxbow-lake biogeochemistry in alluvial plains, mobilization of arsenic, and accumulation in geomorphologically well-defined areas is of paramount importance for the identification of arsenic hotspots and, accordingly, for the implementation of mitigation strategies. To date, the collection and inventory of arsenic-concentration data from tube wells in the shallow-aquifer domain is a tedious and challenging process, given the sheer magnitude of the problem.

The aim of the present study is to construct a conceptual predictive geospatial model for the accumulation of dissolved arsenic as a function of the interaction of oxbow-lake biogeochemistry and alluvial geomorphology. For this, a comprehensive sampling campaign was carried out in and around two oxbow lakes in the floodplain of the Jamuna River Basin in Nadia District, West Bengal, India (23°0′18.89″N, 88°33′55.48″E; Fig. 1A). Water samples were collected from the surface and near the bottom of the oxbow-lake water column for analysis of dissolved organic matter (DOM) and microbial communities. In addition, groundwater samples were collected from shallow and intermediate-depth tube wells in the point bars and levees that border the oxbow lakes (Supplementary Table 1) for analysis of the geospatial distribution of arsenic concentration in the aquifer domain. The results of this study provide a tool for the fast identification of potential arsenic hotspot areas, based on the predictive 'blueprint' model implementation in areas of geomorphological similarity, and thus contribute to a more robust and targeted arsenic mitigation approach.

2. Materials and methods

2.1. Geomorphology

The study location is in a densely-populated area of the Jamuna River Basin in Nadia District, West Bengal, India (average population density in the study area 1093 per km²; Census-2020: https://geoiq.io/places/Nadia/HXkLkDJGM0). Settlements are concentrated on topographically-higher sandy point bars and fluvial levees to provide protection for the population against monsoonal floods. The oxbow lakes surrounding the elevated point bars formed by neck cut-off of meander bends of the Jamuna River in the Lower Ganges Delta of West Bengal. The river was an eastward-flowing, highly-sinuous distributary of the Hooghly River, and in the upper reaches of the Jamuna River Basin the river path has become moribund over time, and detached from the parent river by silting-up as consequence of upstream discharge reduction in the Hooghly River from the 18th Century onward (Mallick, 2013; Sahana et al., 2020). The geomorphology of the Holocene alluvial landscape of the Jamuna River Basin is characterized by flat, low-elevation topography (on average 4 m above mean sea level) of extensive floodplain sandy clay and silt deposits (Sahana et al., 2020). Multiple point-bar and levee sandy deposits stand out as scattered hillocks and ridges up to 8 m above the clayey floodplain landscape (Fig. 1B), as consequence of differential compaction (Sahu and Saha, 2015; Donselaar et al., 2017). Oxbow lakes encompass crescent- and teardrop-shaped point bars on the inner bend of the lake and are fringed by fluvial levees on the outer bend. Ghosh et al. (2021) demonstrated that after detachment from the active river by neck cut-off, oxbow lakes in a similar geomorphological setting along the Ganges River in
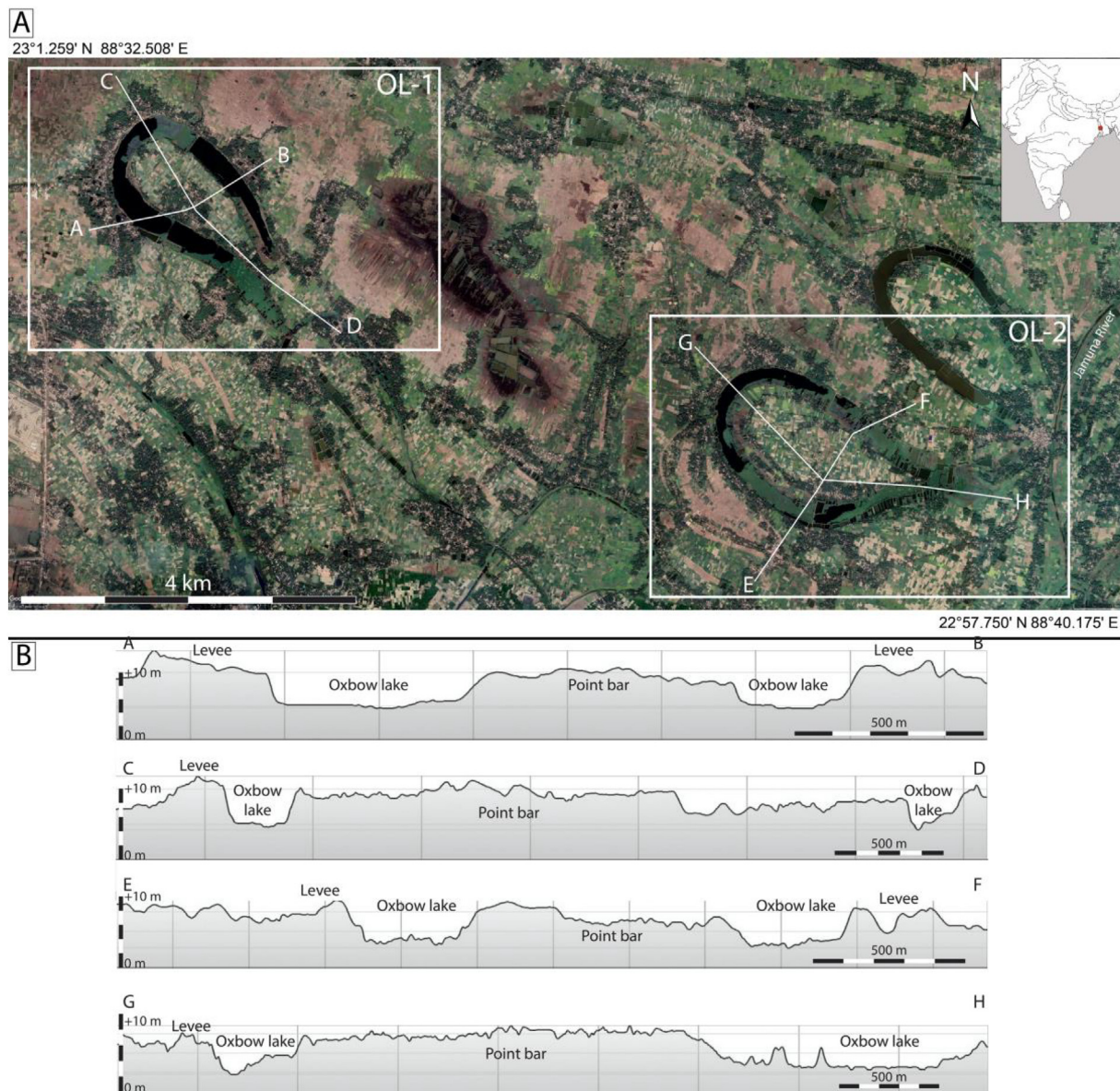
Fig. 1. A) Google-Earth map of study areas OL-1 and OL-2 (image date 6 April 2020). Point bars fringed on all sides by partly-filled oxbow lakes. Jamuna River: largely sediment-filled moribund river path. Curved lines in bottom half and right corner of the image: surface expression of scroll-bar geomorphology. Green patches in the oxbow lake: dense vegetation cover of *Eichhornia crassipes* (water hyacinth). Dark colours to the right of area OL-1: burned after-harvest stubbles. Lines A-B to G-H: cross-section locations of Fig. 1B. B) Cross sections across the study areas.

Bihar are rapidly filled with fine-grained suspension-load sediment (so-called *clay plug*) during monsoonal floods, with a minimum sedimentation rate of 9.6 cm/yr. An estimate of the clay-plug thickness in the present study can be made from bathymetry data of the nearby Hooghly River and the still active part of the Jamuna River east of the study area:

$$H_{clay} = D_{max} - D_{rm} \qquad (1)$$

in which the clay-plug thickness H_{clay} equals the maximum Hooghly River depth D_{max} minus the remnant depth D_{rm} in the partly silted-up Jamuna River. Ghosh et al. (2020) reported a Hooghly River depth of 7 m at 12 km west of the study area. The remnant depth of the Jamuna River on the eastern edge of the study area (Fig. 1A) is 2 m (Mallick, 2013). From these data a clay-plug thickness $H_{clay} = 5$ m can be assumed. The oxbow-lake water is colonized by perennial aquatic macrophytes such as *Eichhornia crassipes* (water hyacinth) and *Hydrilla verticillata* (water thyme) (Ghosh and Biswas, 2015). On satellite imagery, the curved lines on the point bars (Fig. 1A), accentuated by the layout of the agricultural plots, are the surface expression of scroll-bar morphology that consists of alternating inclined layers of clay and sand with a dip toward the river channel (Donselaar et al., 2017). Differential compaction of the two lithology types is expressed by the serrate scroll-bar elevation profile in longitudinal point-bar cross sections (Fig. 1B, profiles C-D and G-H). Upon sediment compaction, the lithological heterogeneity leads to porosity and permeability anisotropy within and between geomorphological units: (a) low-permeable, non-porous clay and silt of the floodplain and (partial) oxbow-lake fill, (b) highly-porous and permeable levee and point-bar sands, and (c) low-permeable, thinly-bedded inclined clay drapes (lateral-accretion surfaces) within the porous and permeable point-bar sands (Donselaar et al., 2017). The clay layers are the expression of the sediment transport and depositional processes in meandering-river bends during flood stage (Miall, 2014). Geogenic arsenic in the sediments of the study area occurs as arsenopyrite and bound in iron-(oxy)hydroxides (Ghosh, 2016; Ghosh et al., 2015b). Porosity and permeability anisotropy between

the geomorphological units has a large impact on groundwater recharge efficiency (c.f., Lasseter et al., 1986) and leads to geospatial variations of arsenic concentrations in the aquifer domain (Van Geen et al., 2008; Nath et al., 2010; Choudhury et al., 2018).

2.2. Sampling strategies

The two study locations (OL-1 and OL-2; Fig. 1A) have a teardrop-shaped point-bar geomorphology with surface areas of 1.1 km^2 and 2 km^2, respectively, completely surrounded by 130 m to 250-m-wide oxbow lakes with an elevated ridge of levee sands on the outer bank. The lakes are largely sediment-filled, converted to agricultural plots, and open sewers drain the remaining surface water functions as open sewers. Groundwater for consumption and irrigation is directly extracted from the porous and permeable point-bar and levee sands via shallow (15–30 m) to intermediate-depth (up to 60 m) tube wells. A total of 109 (52 + 57) georeferenced groundwater samples (ORP between 125 and 150 mV), were collected from existing tube wells in study sites OL-1 and OL-2, respectively (Fig. 1A; Supplementary Table 1) for analysis of the geospatial distribution of arsenic concentration. Tube wells where accessed courtesy of the local owners in the villages, and the sample distribution reflects the village density, with a total of 39 samples in the point-bar areas, and 70 samples on the levees at the outer rim of the oxbow lake/clay plug. Tube-well depths were normalized for the topographical elevation of the well locations (extracted from Google Earth) to elevation above sea level (a.s.l.). The physicochemical parameters (temperature and pH) were measured in situ.

Additionally, to understand the effect of surface derived organic carbon chemistry in inducing microbial growth and metabolism along the water column to the groundwater, bulk water samples were collected from lake water surface (S), lake bottom (B), and groundwater (GW) of OL-1 and OL-2. These samples were used in studying DOC properties (3.3) and microbial metagenomics (3.4).

2.3. Inorganic chemistry analyses

The water samples were collected in triplicate from all locations and filtered through 0.45 μm after acidification. These samples were diluted up to 100 X before quantification in an Inductively Coupled Mass Spectrometer (ICP-MS- Thermo Scientific X-Series II) following Ghosh et al. (2021).

2.4. Organic chemistry analyses

2.4.1. Characterization of low molecular weight (LMW) molecules

2.4.1.1. DOC analyses. The un-acidified raw water samples were collected and stored at 4 °C and used for DIC, DOC (Shimadzu TOC-V CSH analyser), stable carbon isotopes ^{12}C, along with UV$_{254}$ (Agilent Cary Eclipse) and Specific ultraviolet absorbance (SUVA) analyses were made. The specific UV absorbance (SUVA$_{254}$; L/mg·m) was calculated as a ratio of UV$_{254}$ (L/m): DOC (mg/L). The spectrophotometric calibration was done using potassium hydrogen biphthalate (KHP) spiked with NaNO$_3$ (0–100 mg/L) and FeCl$_3$·6H$_2$O (0–3.5 mg/L) added to determine nitrate and ferric iron affecting the absorbance if any.

The samples stored for stable carbon isotopes ^{12}C and ^{13}C were detected on an Isotope Ratio Mass Spectrometer (IRMS) coupled to Gasbench II (Finnigan MAT Delta Plus XL, Germany) with a CTC PAL-80 autosampler and the ratio

$$\delta^{13}C = \left\{ \frac{\left(^{13}C/^{12}C \right)_{sample}}{\left(^{13}C/^{12}C \right)_{reference}} \right\} \times 100 \qquad (2)$$

(δ^{13}CDIC) of DIC was determined following Assayag et al. (2006) [per mil (‰); Eq. (2)] with respect to the reference standard Vienna Pee Dee Belemnite (V-PDB):

2.4.2. Characterization of high molecular weight (HMW)-DOM

2.4.2.1. Alkane and sterol hydrocarbons. The characterization of *n*-alkanes was done by collecting the OC on ENVITM C-18 SPE DSK (C-18 bonded silica; Sigma–Aldrich) discs from the water samples collected (detailed in Ghosh et al., 2021). The lipid fractions were extracted using dichloromethane (DCM) and methanol mixture (9:1 *v*/v) using ultra-sonication (Wu et al., 2014) and quantified (GC–MS parameters) as per Ghosh et al. (2015b).

2.5. Microbiological analyses

2.5.1. Metagenomics

For the microbial community profiling, the water samples were collected from 12 different locations of the bottom of the lakes and 12 different groundwater sampling points around both lakes. The biomass was recovered by filtering 2 L of the water sample through 0.22 μm filter (milipore). All the filters were stored at −80 °C and were later used for environmental DNA extraction using the DNeasy UltraClean microbial kit (Qiagen). Afterward, the DNA samples were sent for metagenomics analysis at AgriGenome Labs Pvt. Ltd., India. The amplification of the V3-V4 region of 16S rRNA genes were performed using the universal primers 341F (5′- CCT ACG CGA GGC AGC AG −3′) and 517r (5′- ATT ACC GCG GCT GG −3′) (Muyzer et al., 1993). Polymerase chain reactions (PCR) were performed with Phusion® High-Fidelity PCR Master Mix (New England Biolabs). The same volume of 1× loading buffer was mixed (containing SYBR green) with PCR products and electrophoresis on 2 % agarose gel electrophoresis was performed for detection. Samples with a bright prominent band strip between size 400–450 bp were chosen for further experiments. The PCR products were mixed in equal ratios and purified with the Qiagen Gel Extraction Kit (Qiagen, Germany). The Illumina HiSeq paired-end raw reads were generated with NEBNext® UltraTM DNA Library Prep Kit and quantified via Qubit.

The Illumina HiSeq paired-end raw reads were checked for quality (Base quality, base composition, GC content) using the FastQC tool (Andrews, 2010). The QIIME (Version: 1.9.1) pipeline (Caporaso et al., 2010) was used for the selection of 16S RNA, clustering, and Operational Taxonomic Unit (OTU) picking. The chimeric sequences were removed from the libraries using the de-novo chimera removal method UCHIME implemented in the tool VSEARCH. Pre-processed reads from all samples were pooled and clustered into OTUs, based on their sequence similarity using the Uclust program (similarity cutoff = 0.97). A representative sequence was identified for each OTU and aligned against the SILVA core set of sequences using the PyNAST program (Caporaso et al., 2010). The representative sequences of the OTUs were also used to predict KEGG orthodoxy (KO) abundances using PICRUSt2 (Douglas et al., 2020) and microbial pathways were inferred. The 24 metagenomic library datasets from were clustered, based on the arithmetic mean of weighted Unifrac distance using Unweighted Pair Group Method (UPGMA). The clustered OTUs were distributed into four sampling conditions (OL-1 bottom, OL-2 bottom, OL-1 groundwater and OL-2 groundwater). The raw sequencing data have been submitted to the NCBI Sequence Read Archive; accession number PRJNA603427 (https://www.ncbi.nlm.nih.gov/sra/PRJNA603427).

2.5.2. MPN test for coliform detection

To detect the sewage inputs from the local villages into the lake waters, the coliform load in the water samples was detected using the classic Most probable Number (MPN) test (Oblinger and Koburger, 1975), using Mac-Conkey broth with the dye Bromo cresol purple (5′, 5″-dibromo-o-cresol sulfophthalein, Hi Media) with Duhram's tube inserts to detect gas bubbles.

2.5.3. Microcosm lability test (MLT)

Eleven arsenic oxidizing bacterial strains were isolated from the oxbow lake water samples and were identified by 16S rRNA gene sequencing [GenBank accession no. MW383510 to MW383925]. A Neighbour Joining tree (Fig. 2A) was prepared using MEGA version 10.0 (X) (Stecher et al., 2020), following the sequencing and bioinformatic methods detailed in Chikkanna et al. (2018, 2021).
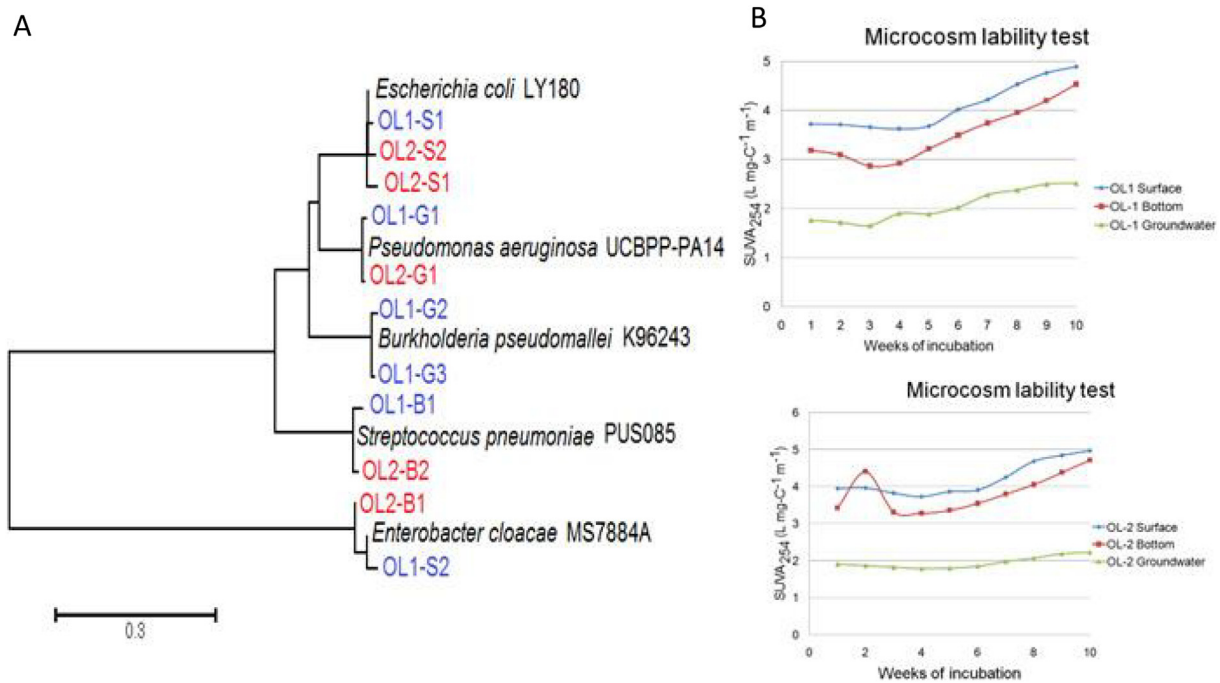
Fig. 2. The Microcosm Lability Test (MLT): A) An NJ Tree to understand the taxonomy if the isolated bacterial genera participated in the MLT. The blue coloured strain names are the one isolated from OL-1 and the red coloured are strains from OL-2. B) the graphs indicate the utilization of faster utilization of the available DOC represented by $SUVA_{254}$ in both the lakes.

A homogenous mixture of the isolated microbial strains at the log phase of growth was used as inoculum (1 % v/v) to test their metabolic efficiency to degrade the DOC. The organic molecules were collected using ENVI™ C-18 DSK (C-18 bonded silica; Sigma–Aldrich) from water samples collected from the lake surface, lake bottom and groundwater borehole of OL-1 and OL-2. The microcosms were established providing minimal salt based media pH 7.2 inoculated with the above inoculum (1 % v/v) and incubated for 10 weeks and the lability of DOC were tested based on the change in $SUVA_{254}$ quantification (Fig. 2B).

3. Results

3.1. Organic chemical proxies

The DOC values of lake bottom water ranged from 1294 to 2138 mg/L, and were lower in the groundwater samples. The average $\delta^{13}C$ value of the water samples was -23 ‰ and average $\delta^{15}N$ was 4.13 ‰.

The total *n*-alkane abundance in the lake bottom samples varied from 529 to 8962 ng/L. All the samples showed a bimodal distribution where
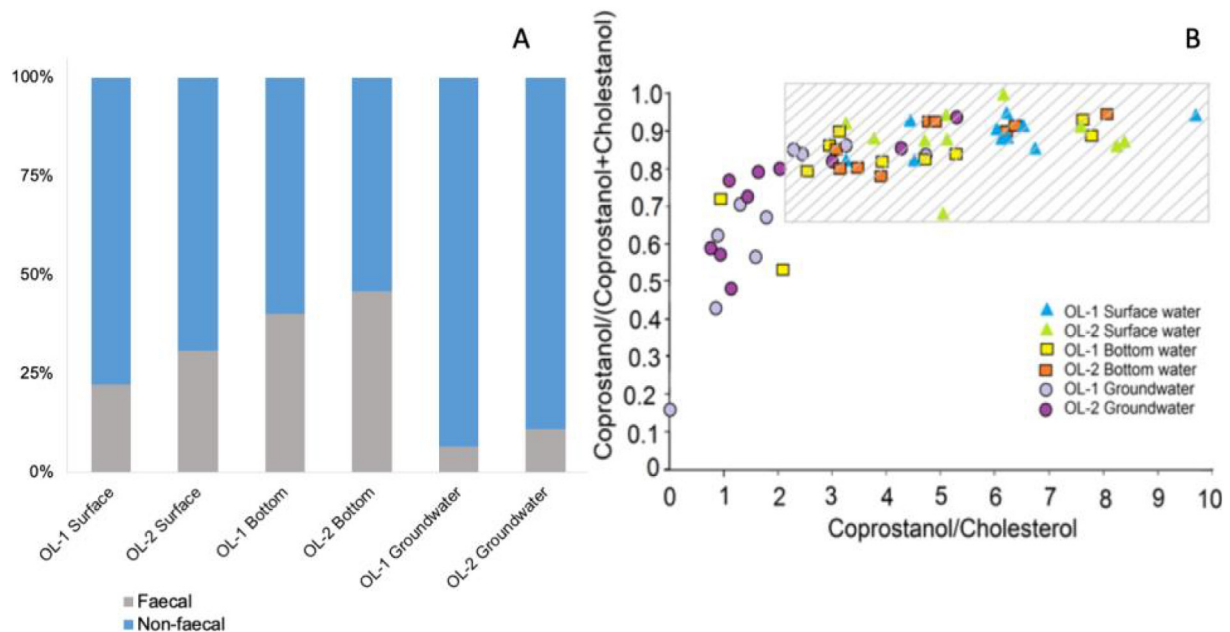
Fig. 3. A) The % abundance of sterol source Faecal vs Non-Faecal. B. Relative contribution of (Σ Coprostanol + 24-Ethylcoprostanol + Epicoprostanol + Sitostanol) vs total sterol abundance. B) The ratio of Coprostanol / (Coprostanol + Cholestanol) as a function of the Coprostanol/ Cholestanol ratio (Reichwaldt et al., 2017). The shaded area represents faecal contamination identified by both ratios.

both the low molecular weight (LMW) (C_{13} to C_{21}) and high molecular weight (HMW) (C_{23} to C_{35}) n-alkanes were equally dominant. However, in the groundwater samples the predominance of HMW n-alkanes was observed. The specific sterol markers were used to understand the hypothesis of this study and are described below.

A predominant abundance of odd alkane hydrocarbons was observed in all the lake bottom samples. To predict the sources of these hydrocarbons, various ratios were used. The modified Carbon Preference Indexes (CPI) for aquatic samples predicted by Ghosh et al. (2015a) as CPI$_{TOT}$ (nC_{13} to nC_{35}; Eq. (3)), CPI$_{LMW}$ (nC_{13} to nC_{21}; Eq. (4)) and CPI$_{HMW}$ (nC_{23} to nC_{35}; Eq. (5)) [Eqs. (2), (3), (4)]. The CPI$_{TOT}$ (ranged from 6.37 to 7.92) and CPI$_{HMW}$ (ranged from 3.13 to 24.09) were higher in the bottom water from all the sites, whereas CPI$_{LMW}$ (ranged from 3.72 to 5.24) was high in surface water.

$$CPI_{TOT} = \frac{\Sigma(C_{13} \text{ to } C_{33})_{odd} + \Sigma(C_{15} \text{ to } C_{35})_{odd}}{2\Sigma(C_{14} \text{ to } C_{34})_{even}} \tag{3}$$

$$CPI_{LMW} = \frac{\Sigma(C_{13} \text{ to } C_{19})_{odd} + \Sigma(C_{15} \text{ to } C_{21})_{odd}}{2\Sigma(C_{14} \text{ to } C_{20})_{even}} \tag{4}$$

$$CPI_{HMW} = \frac{\Sigma(C_{23} \text{ to } C_{33})_{odd} + \Sigma(C_{25} \text{ to } C_{35})_{odd}}{2\Sigma(C_{24} \text{ to } C_{34})_{even}} \tag{5}$$

The sewage biomarkers such as Coprostanol, 24-Ethylcoprostanol, Epicoprostanol, and Sitostanol were detected at relatively higher abundance (25 to 45 %) in the lake water samples (which reduces but persists in the groundwaters as well, tracing the sewage flow into the aquifers (Fig. 3).

The groundwater samples from both OL-1 and OL-2 had signatures that are processed in maturation, whereas the in lake water samples only 92.2 % of the facultative, and only 11 % of the maturation samples were identified as containing faecal contamination (Fig. 3A).

The ratio Coprostanol / (Coprostanol + Cholestanol) is used as a function of the ratio Coprostanol / Cholesterol (Reichwaldt et al., 2017), to further understand the distribution of the sewage biomarkers in the samples. The correlation of these two sterol ratios (Fig. 3B) was used to differentiate between human sterols and the sterols from other biogenic sources:

ΣCoprostanol/(ΣCoprostanol + ΣCholestanol) vs (ΣCoprostanol/ΣCholesterol).

The shaded area (Fig. 3B) represents faecal contamination identified by both of the ratios, support the inferences of this work. The abundance is highest in the surface water of the lakes, which are reduced by microbial oxidation in the lake bottom however, these markers still remain trackable in the groundwater samples (Fig. 3).

3.2. Microbial metabolism analyses

The metagenomic analysis of the lake bottom water indicated a predominance of OTUs represented by methylotrophes (*Methylophillaceae*), along with iron oxidizing- arsenate reducing bacterial classes like *Gallionellaceae, Pseudomonadaceae, Sphingomonadaceae* and *Nocardiodes* (Fig. 4). The
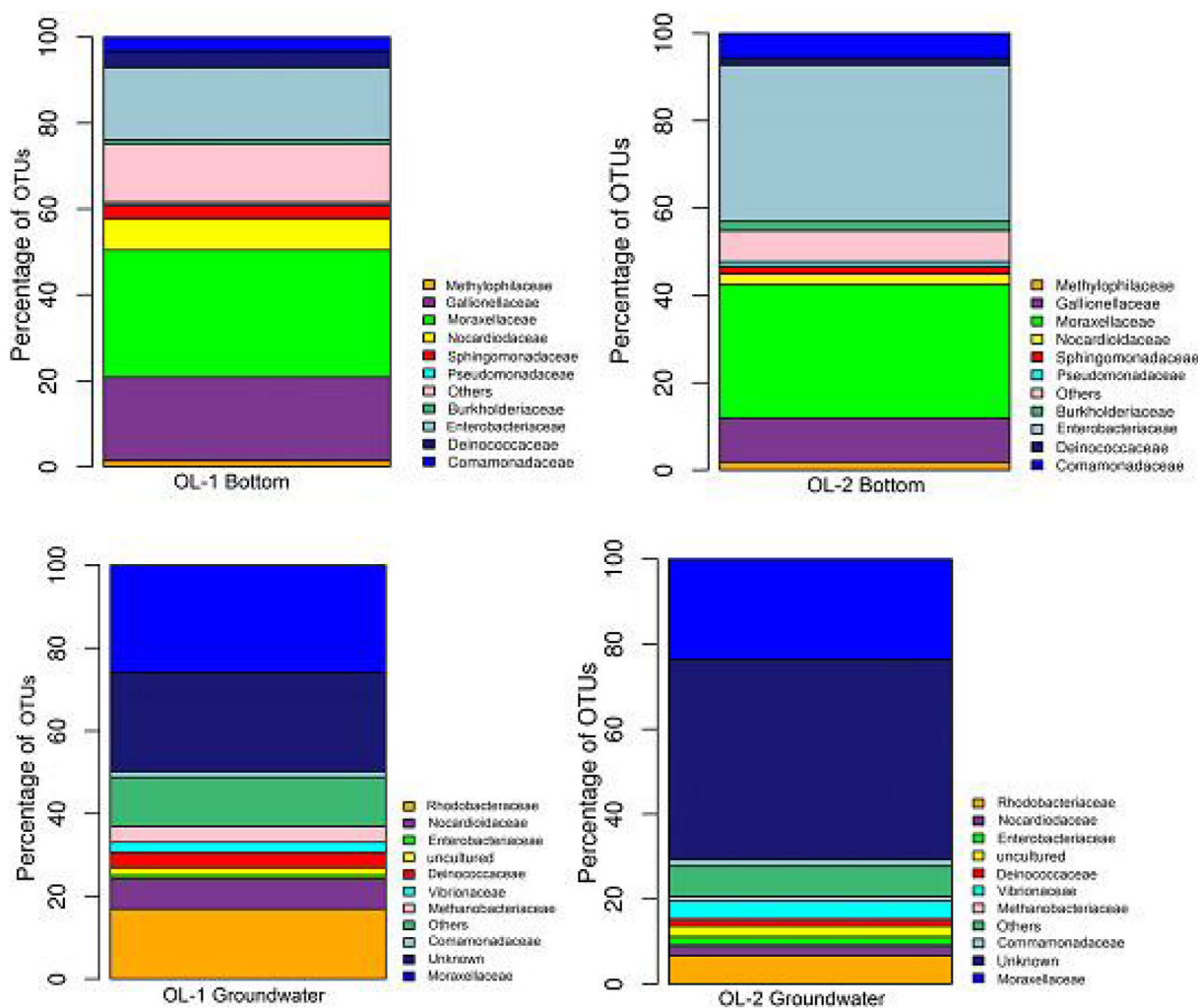

Fig. 4. Distribution and percentage abundance of predominant OTUs representing microbial classes. Each column represents six metagenomic library data of the V3-V4 region of 16S rRNA. A) The columns represents the water samples collected from the bottom of the two lakes OL-1 and OL-2. B) The column represents the water samples collected from the groundwater boreholes around the oxbow lakes.

methane metabolism is also indicated by the PICRUSt analysis (Fig. 5). The absence of sulphate reducing groups despite of faecal contamination could trigger the enhanced reductive dissolution of arsenopyrite and As-bound with Fe(*oxy*)hydroxides. Interestingly 5–8 % of the OTU abundance consisted of enteric-microflora like *Enterobacteriaceae* (Fig. 4) in both lake water indicating high amount of sewage disposal in the lakes.

In the groundwaters, the OTUs represented by arsenate reducers such as *Pseudomonas, Shewanella*, along with the iron and arsenite oxidizers such as *Acinetobacter, Burkholderia* were detected and 0.8 to 4 % of the OTUs representing faecal derived microbial groups such as the class *Enterobacteriaceae*. The abundance of the coliform is further confirmed by the MPN test. Interestingly, various iron-oxidizing groups that can co-metabolize arsenic were detected (Ghosh et al., 2018). The Nitrate dependent Fe-oxidizers (NDFOs) such as *Rhodobacteriaceae*, other Fe-oxidizers like *Nocardiodaceae* and dissimilatory iron reducers such as *Moraxellaceae* were found to be dominant in the groundwater.

To understand if the faecal derived OTUs are functional in the representative samples, the MPN test was performed, which indicated a high coliform abundance in the surface and groundwater samples. The surface/lake bottom water (11 to 17×10^2 coliforms/mL) had a higher count relative to a small reduction in the groundwaters (4 to 9×10^2 coliforms/mL), which could be due to the dilution effect.

The Microcosm Lability Test (MLT) indicates a depletion in $SUVA_{254}$ values from the surface to the bottom of the lake and further in the groundwater in both sampling stations (Fig. 2). This suggests that the total aromatic content of the DOC is bioavailable, reactive and quickly consumed by the groundwater microbial flora. The hydropedological properties of the aquifer sediments allow the vertical movement (through leaching and percolation) of the organic molecules and microbial communities along the water column.

3.3. Geospatial distribution of arsenic

The geospatial distribution of arsenic concentrations in groundwater shows a clear relation with the alluvial geomorphology (Figs. 6–7). The oxbow lake and its partial clay-plug fill marks a boundary between arsenic concentrations with highest concentrations, averaging 505 μg/L (Fig. 7A) in the confined space of point bars surrounded on all sides by an oxbow-lake/clay plug, and areas beyond the oxbow-lake confinement with concentrations that average 121 μg/L, i.e., a factor 4.1 lower than those in the point-bar aquifer. The concentration distribution shows a random pattern with depth of the tube wells (Fig. 7B).

4. Discussion

4.1. Interactions of oxbow-lake biogeochemistry and alluvial geomorphology

Our study shows that anoxic oxbow lakes and clay plugs, rich in labile organic matter, act as an efficient factory for the mobilization of arsenic by microbially-mediated reductive dissolution. The oxbow lakes are sinks to natural organic carbon that accumulates in the form of HMW-DOC (Ghosh et al., 2021; Cao et al., 2022), and also for the anthropogenic organic matter as depicted in this case. The relatively high abundance of those HMW-DOC indicated by high CPI_{HMW} but low CPI_{TOT} also suggest the microbial digestion and utilization (Ghosh et al., 2015a). Additionally the faecal-derived tracers (Coprostanol and Coprostenols) suggest enrichment of the surface and groundwater with C and N sources (Kriaa et al., 2019). Such large pool of rich C-sources provides perfect incubation
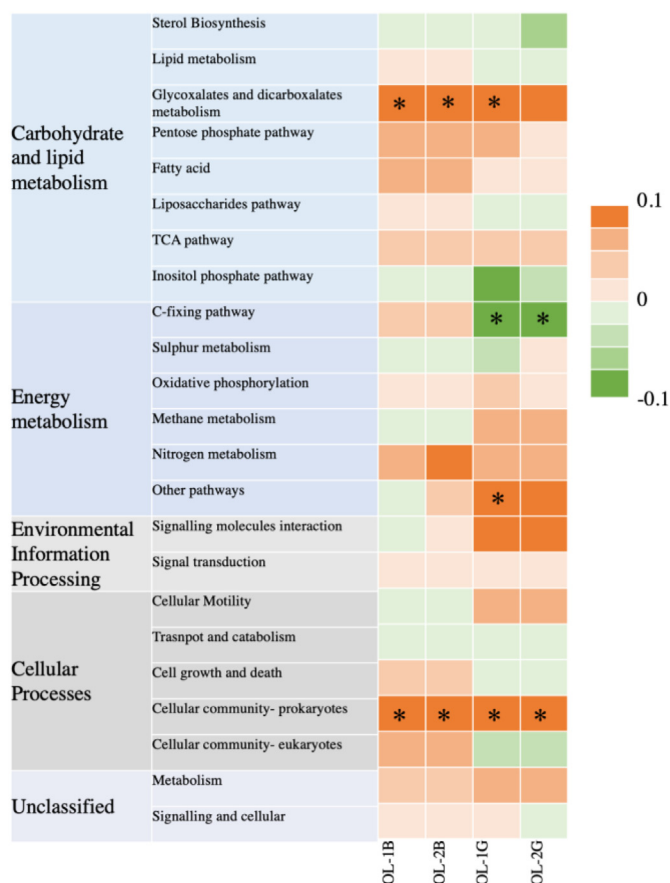
Fig. 5. Microbial PICRUSt-predicted KEGG functions relevant to metabolism in the metagenomic library datasets. The heatmap denotes the direction of association between each microbial PICRUSt-predicted KEGG function and arsenic metabolism based on the scale given on the right. The significant associations are highlighted with '*'.
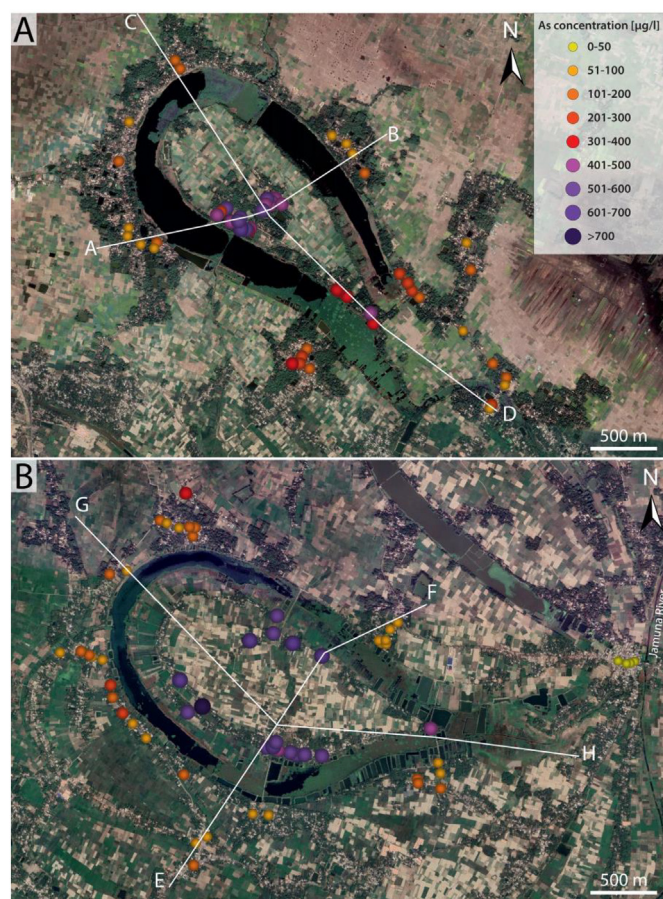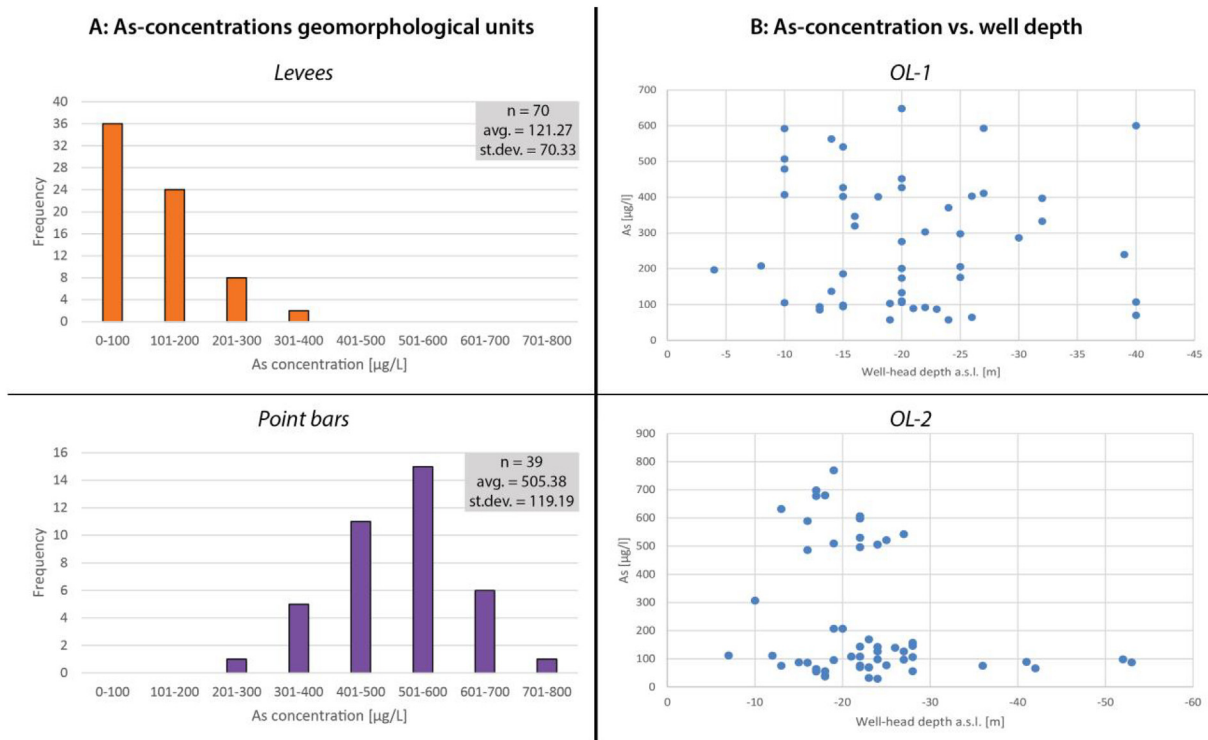
Fig. 6. Geospatial distribution of groundwater arsenic concentrations in tube wells of areas OL-1 (A) and OL-2 (B). Lines A-B to G-H: cross-section locations of Fig. 1B.
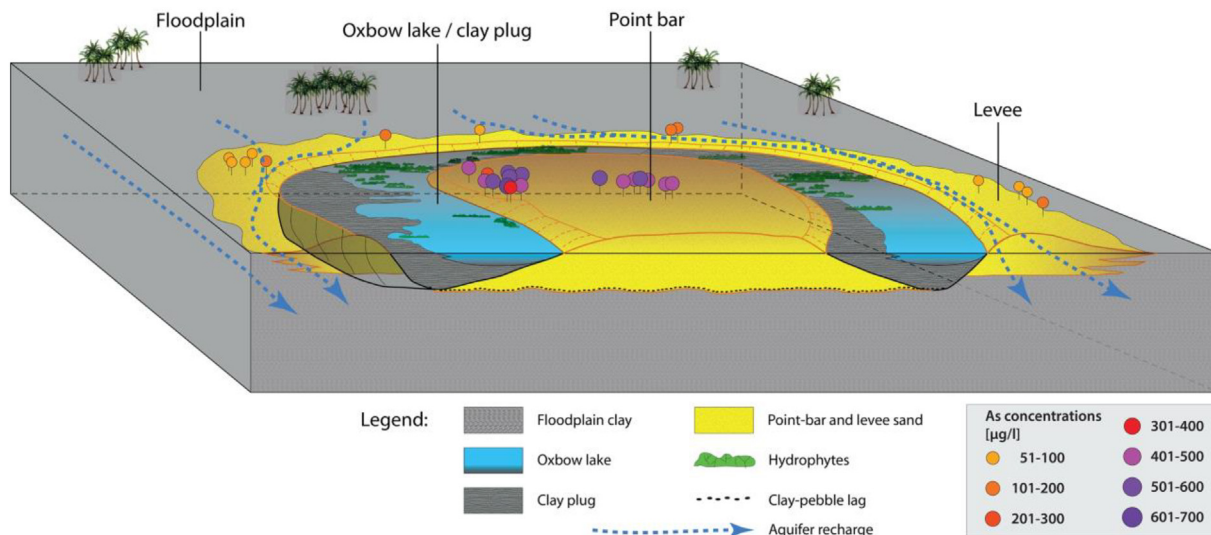
Fig. 7. (A) Groundwater arsenic concentrations in levees outside the oxbow-lake confinement, and in the point-bars encompassed by oxbow lakes. (B) Cross-plots of arsenic concentrations vs. tube-well depth. Well depths normalized to height above sea level (a.s.l.).

condition for facultative methanogens (Glodowska et al., 2020). During the transportation of this DOM pool into the aquifers a fractionation occurs with a function of molecular weight and recalcitrance, as depicted in the chromatographic model by Ghosh et al. (2021). Such accumulation of HMW-DOM can also cause increased mobilization of arsenic in anoxic aquifer systems (Wu et al., 2019; Glodowska et al., 2020).

Microbial mobilization takes place in the aqueous phase (i.e., in the remnant oxbow lake water), and in the sediment of the clay plug. Dissolved arsenic in the oxbow lake migrates by water percolation into the adjacent porous and permeable point-bar and levee sands. Upon microbial mobilization in the clay-plug sediment, (pathways indicated in Fig. 8), the dissolved arsenic migrates along the porosity-permeability gradient and accumulates

in juxtaposed porous and permeable point-bar and levee sands by the processes of gravitational, compaction-driven diffusion in the clay plug, and transport-driven advection past the permeability boundaries at the interface of clay-plug to point-bar, and clay-plug to levee (Kumar et al., 2021a).

In an unconfined isotropic subsurface, the accumulated arsenic concentrations would be diluted by the regional groundwater flux from the Ganges Delta to the Bay of Bengal (Basu et al., 2001; Harvey, 2002; Mukherjee et al., 2007; Sikdar and Chakraborty, 2017). In the Holocene alluvial landscape, porosity and permeability anisotropy within and between the alluvial geomorphological elements conditions the recharge efficiency (Fig. 8). The clay-plug sediment of the partially-filled oxbow lake surrounding the point-bar deposits on all sides acts as aquitard and creates a

Fig. 8. Conceptual geospatial model of the relation between geomorphological porosity-permeability anisotropy, arsenic-concentration differences, and regional groundwater flow. Arsenic-pin locations are those of Fig. 6A.

geomorphological entrapment of groundwater in the point-bar sands (Fig. 8, Graphical Abstract).

In the present study no additional cored wells were drilled. As the process of sediment transport and accumulation on the inner bank of a meander bend in any meandering-river is controlled by the helicoidal flow in the water column of the river (Friend et al., 1996), it can readily be assumed that the point-bar geomorphology and internal sedimentary architecture are similar to that described from cores further upstream, along the Ganges River in Bihar, India (Donselaar et al., 2017; Kumar et al., 2021a), and conform with the 'classic' point-bar sedimentary architecture, characterized by a coarse-grained clean-sand base, internal point-bar heterogeneity, such as the upward-fining grain-size trend and the occurrence of intermittent thin, inclined clayey lateral-accretion surfaces in point-bar sands (Donselaar and Overeem, 2008; Donselaar et al., 2017). The inherent porosity and permeability anisotropy in the point-bar geomorphological element limits groundwater recharge by the regional groundwater flux. Consequently, arsenic contamination in the enclosed point-bar aquifer is not diluted and remains high. By contrast, fluvial levees are elongate, ribbon-shaped sandy geomorphological units (wedge-shaped in cross-section) that fringe the oxbow lake over its entire length, (c.f. Branß et al., 2022), lack internal permeability contrast and are not confined on all sides by impermeable clay, resulting in a much more efficient aquifer flushing and decrease of arsenic concentrations.

4.2. Predictive geospatial modelling

The depth of the geomorphological groundwater entrapment in recent alluvial deposits equals the thickness of the individual point-bar – oxbow-lake geomorphological-element couple, and scales with the depth of the river from which they originate. Maximum depth data of the Jamuna River in the study area are not readily available because of the moribund state of the river (Mallick, 2013; Sahana et al., 2020), and bathymetric data of the Hooghly River, of which the Jamuna River was a distributary, serve as proxy. Measured river depth in a stretch 12 km west of the study area (Ghosh et al., 2020) is 7 m, which would be an indication of the entrapment depth. From this an estimate can be made of the arsenic mass contained in a single, enclosed point-bar – oxbow-lake geomorphological-element couple as:

$$M_{As} = BSV * N/G * \Phi \qquad (6)$$

where M_{As} is the potential arsenic mass, BSV the bulk sediment volume of the point-bar geomorphological unit confined by a clay plug, N/G the net-to-gross of the point-bar unit, and Φ the porosity. The potential arsenic mass of the point-bars in the present study is $0.62 * 10^6$ to $1.13 * 10^6$ kg (Supplementary Table 2).

The uppermost, recent alluvial sediment is part of the Holocene Ganges alluvial-valley fill with a maximum thickness of 90 m (Goodbred and Kuehl, 2000a, 2000b). Hence, the arsenic hotspots in local point-bar – oxbow-lake aquifer confinements will not be limited to the uppermost, recent alluvial deposits, and will extend down throughout the Holocene depositional succession of the Ganges valley fill. Goodbred and Kuehl (2000b) interpreted the succession as stacked fluvial and floodplain deposits, and it is proposed here that the fluvial channel sands therein are point-bar geomorphological elements, as these have the best preservation potential in the meandering-river environment (Donselaar and Overeem, 2008; Parquer et al., 2020). The assumption that the arsenic contamination extends down in the depositional succession is confirmed by the cross-plot of groundwater arsenic against well depth (Fig. 7B) that shows no decreasing trend of concentration with depth. From this it is interpreted that arsenic can freely percolate throughout the entire 60 m well-penetration depth in the subsurface in the study area in the absence of horizontal aquitards. The interpretation is sustained by arsenic concentration values of previous studies in Nadia District (West Bengal), where Bhattacharya et al. (2001) reported arsenic concentrations of 10–350 µg/L in tube wells of 80 m to more than 150 m deep; and high arsenic concentrations (to 475 µg/L) are found in 20 m to 30-m-deep tube wells west of the Hooghly River (Mukherjee et al., 2010).

In summary, this study allows for the construction of a predictive geospatial model, in which the point-bar – oxbow-lake geomorphological-element couple is identified as arsenic hotspot, and the partly clay-filled oxbow lake plays a dual role as factory for the microbial reductive dissolution of arsenic in an anoxic environment rich in labile organic matter, and as aquitard that effectively shields the aquifer recharge in porous point-bar sand on the condition that the oxbow lake forms a closed loop around the point bar. High population density on the point-bar higher grounds combined with sub-optimal sanitation conditions further aggravate the arsenic problem. It is proposed here to build predictive geospatial models by integrating remotely-sensed satellite imagery and digital elevation data of the Holocene alluvial-plain geomorphology in combination with GIS-based population databases and machine learning techniques (Connolly et al., 2021). The models can be applied on a global scale for the identification of large swats of arsenic hotspots in arsenic-affected Holocene alluvial plains in a comparable climate and geomorphological setting.

5. Conclusions

In the present study it is demonstrated that oxbow lakes and corresponding clay plugs of the Holocene alluvial landscape in the Lower Ganges Delta comprise an anoxic environment, rich in labile organic matter (natural and anthropogenic) that acts as efficient factory for the mobilization of arsenic by microbially-mediated reductive dissolution. More specifically, the abundant occurrence of natural and anthropogenic (faecal-derived) organic matter in clay-plug sediment favours microbial digestion and utilization, and arsenic mobilization.

The dissolved arsenic migrates to and accumulates in adjacent porous and permeable point-bar and levee sands. Large As-concentration differences (505 µg/L on average in point bars vs. 121 µg/L in the levees) are attributed to the clay-plug aquitard, which creates groundwater entrapment in the encompassed point-bar sands. In this geomorphologically-confined space, arsenic-laden groundwater is shielded from dilution by the regional groundwater flux from the Ganges Delta to the Bay of Bengal. By contrast, fluvial levees beyond the oxbow lake are not confined on all sides by a clay-plug, resulting in a much more efficient aquifer flushing and decrease of arsenic concentrations. On the basis of the point-bar size in the study area, and the average groundwater arsenic content, the potential total arsenic load per point bar is in the order of $0.62 * 10^6$ to $1.13 * 10^6$ kg. Arsenic can freely percolate throughout the entire 60 m well-penetration depth in the subsurface in the study area in the absence of horizontal aquitards.

The occurrence of well-defined arsenic hotspots by synergy of biogeochemical processes and alluvial geomorphology opens up opportunities for creating predictive GIS-based geospatial models for the global-scale identification of large swats of arsenic hotspots in arsenic-affected Holocene alluvial plains.

CRediT authorship contribution statement

DG – Conceptualization, Methodology, Investigation (Data collection and formal analysis), Writing – original draft, Funding acquisition.
MED – Conceptualization, Methodology, Investigation (Data collection and formal analysis), Writing – original draft, Funding acquisition.

Data availability statement

The data that support the findings of this study are available on request from the corresponding author.

Declaration of competing interest

The authors declare that they have no known competing financial interests or personal relationships that could have appeared to influence the work reported in this paper.

Acknowledgements

Appendix A. Supplementary data

Supplementary data to this article can be found online at https://doi.org/10.1016/j.scitotenv.2022.158952.

References

Acharyya, S.K., Shah, B.A., 2007. Groundwater arsenic contamination affecting different geologic domains in India—a review: influence of geological setting, fluvial geomorphology and quaternary stratigraphy. J. Environ. Sci. Health Part A 42, 1795–1805.

Acharyya, S.K., Lahiri, S., Raymahashay, B.C., Bhowmik, A., 2000. Arsenic toxicity of groundwater in parts of the Bengal basin in India and Bangladesh: the role of quaternary stratigraphy and Holocene Sea-level fluctuation. Environ. Geol. 39, 1127–1137.

Ahmed, K.M., Bhattacharya, P., Hasan, M.A., Akhter, S.H., Alam, S.M.M., Bhuyian, M.A.H., Imam, M.B., Khan, A.A., Sracek, O., 2004. Arsenic contamination in groundwater of alluvial aquifers in Bangladesh: an overview. Appl. Geochem. 19, 181–200. https://doi.org/10.1016/j.apgeochem.2003.09.006.

Andrews, S., 2010. FastQC: a quality control tool for high throughput sequence data. Available online at http://www.bioinformatics.babraham.ac.uk/projects/fastqc/.

Assayag, N., Rivé, K., Ader, M., Jézéquel, D., Agrinier, P., 2006. Improved method for isotopic and quantitative analysis of dissolved inorganic carbon in natural water samples. Rapid Commun. Mass Spectrom. 20, 2243–2251. https://doi.org/10.1002/rcm.2585.

Aziz, Z., van Geen, A., Versteeg, R., Horneman, A., Zheng, Y., Goodbred Jr., S.J., Ahmed, K.M., 2008. Impact of local recharge on arsenic concentrations in shallow aquifers inferred from the electromagnetic conductivity of soils in Araihazar, Bangladesh. Water Resour. Res. 44, W07416. https://doi.org/10.1029/2007WR006000.

Basu, A.R., Jacobsen, S.B., Poreda, R.J., Dowling, C.B., Aggarwal, P.K., 2001. Large groundwater strontium flux to the oceans from the Bengal Basin and the marine strontium isotope record. Science 293 (5534), 1470–1473. https://doi.org/10.1126/science.1060524.

Berg, M., Stengel, C., Trang, P.T.K., Hung Viet, P., Sampson, M.L., Leng, M., Samreth, S., Fredericks, D., 2007. Magnitude of arsenic pollution in the Mekong and Red River Deltas - Cambodia and Vietnam. Sci. Total Environ. 372, 413–425. https://doi.org/10.1016/j.scitotenv.2006.09.010.

BGS, DPHE, 2001. Arsenic contamination of groundwater in Bangladesh. In: Kinniburgh, D.G., Smedley, P.L. (Eds.), British Geol. Surv. Rep. WC/00/19. 1. British Geol. Surv., Keyworth, U.K, pp. 1–21.

Bhattacharya, P., Jacks, G., Jana, J., Sracek, A., Gustafsson, J.P., Chatterjee, D., 2001. Geochemistry of the Holocene alluvial sediments of Bengal Delta Plain from West Bengal, India: implications on arsenic contamination in groundwater. In: Jacks, G., Bhattacharya, P., Knan, A.A. (Eds.), Groundwater arsenic contamination in the Bengal Delta Plain of Bangladesh. KTH Spec. Publ., TRITA-AMI Report 3084, pp. 21–40.

Bhattacharya, P., Claesson, M., Bundschuh, J., Sracek, O., Fagerberg, J., Jacks, G., Martin, R.A., Storniolo, A., Thir, J.M., 2006. Distribution and mobility of arsenic in the Río Dulce alluvial aquifers in Santiago del Estero Province,Argentina. Sci. Total Environ. 358, 97–120. https://doi.org/10.1016/j.scitotenv.2005.04.048.

Branß, T., Núñez-González, F., Aberle, J., 2022. Fluvial levees in compound channels: a review on formation processes and the impact of bedforms and vegetation. Environ. Fluid Mech. 1–27. https://doi.org/10.1007/s10652-022-09850-9.

Bundschuh, J., Farias, B., Martin, R., Storniolo, A., Bhattacharya, P., Cortes, J., Bonorino, G., Albouy, R., 2004. Groundwater arsenic in the Chaco-Pampean Plain, Argentina: case study from Robles county, Santiago del Estero Province. Appl. Geochem. 19, 231–243. https://doi.org/10.1016/j.apgeochem.2003.09.009.

Campbell, J.R., Craw, D., Frew, R., Horton, T., Chamberlain, C.P., 2004. Geochemical signature of orogenic hydrothermal activity in an active tectonic intersection zone, Alpine Fault, New Zealand. Mineral. Deposita 39, 437–451. https://doi.org/10.1007/s00126-004-0421-4.

Cao, W., Guo, H., Zhang, Y., Ma, R., Li, Y., Dong, Q., Li, Y., Zhao, R., 2018. Controls of paleochannels on groundwater arsenic distribution in shallow aquifers of alluvial plain in the Hetao Basin, China. Sci. Total Environ. 613–614, 958–968. https://doi.org/10.1016/j.scitotenv.2017.09.182.

Cao, W., Gao, Z., Guo, H., Pan, D., Qiao, W., Wang, S., Ren, Y., Li, Z., 2022. Increases in groundwater arsenic concentrations and risk under decadal groundwater withdrawal in the lower reaches of the Yellow River basin, Henan Province China. Environ Pollut. 296, 118741. https://doi.org/10.1016/j.envpol.2021.118741.

Caporaso, J., Kuczynski, J., Stombaugh, J., et al., 2010. QIIME allows analysis of high-throughput community sequencing data. Nat. Methods 7, 335–336. https://doi.org/10.1038/nmeth.f.303.

Chakraborti, D., Rahman, M.M., Das, B., Nayak, B., Pal, A., Sengupta, M.K., Hossain, M.A., Ahamed, S., Sahu, M., Saha, K.C., Mukherjee, S.C., Pati, S., Dutta, R.N., Quamruzzaman, Q., 2013. Groundwater arsenic contamination in Ganga-Meghna-Brahmaputra plain, its health effects and an approach for mitigation. Environ. Earth Sci. 70, 1993–2008. https://doi.org/10.1007/s12665-013-2699-y.

Chikkanna, A., Ghosh, D., Kishore, A., 2018. Expression and characterization of a potential exopolysaccharide from a newly isolated halophilic thermotolerant bacteria Halomonas nitroreducens strain WB1. PeerJ 6, e4684. https://doi.org/10.7717/peerj.4684.

Chikkanna, A., Mehan, L., Sarath, P.K., Ghosh, D., 2019. Arsenic exposures, poisoning, and threat to human health: arsenic affecting human health. In: Papadopoulou, P., Marouli, C., Misseyanni, A. (Eds.), Environmental Exposures and Human Health Challenges, 1st ed. IGI Global, pp. 86–105 https://doi.org/10.4018/978-1-5225-7635-8.ch004.

Chikkanna, A., Ghosh, D., Sajeev, K., 2021. Bio-weathering of granites from Eastern Dharwar Craton (India): a tango of bacterial metabolism and mineral chemistry. Biogeochemistry 153, 303–322. https://doi.org/10.1007/s10533-021-00791-x.

Choudhury, R., Nath, B., Khan, M.R., Mahanta, C., Ellis, T., van Geen, A., 2018. The impact of aquifer flushing on groundwater arsenic across a 35-km transect perpendicular to the upper Brahmaputra River in Assam, India. Water Resour. Res. 54, 8160–8173. https://doi.org/10.1029/2017WR022485.

Connolly, C.T., Stahl, M.O., DeYoung, B.A., Bostick, B.C., 2021. Surface flooding as a key driver of groundwater arsenic contamination in Southeast Asia. Environ. Sci. Technol. 56, 928–937. https://doi.org/10.1021/acs.est.1c05955.

Das, A., Mondal, S., 2021. Geomorphic controls on shallow groundwater arsenic contamination in Bengal basin, India. Environ. Sci. Pollut. Res. 28, 42177–42195. https://doi.org/10.1007/s11356-021-13761-5.

Das, D., Chatterjee, A., Samanta, G., Mandal, B., Chowdury, T.R., Samanta, G., Chowdury, P.P., Chanda, C., Basu, G., Lodh, D., Nandi, S., Chakraborty, T., Mandal, S., Bhattacharya, S.M., Chakraborti, D., 1994. Arsenic contamination in groundwater in six districts of West Bengal, India: the biggest arsenic calamity in the world. Analyst 119, 168N–170N. https://doi.org/10.1039/AN994190168N.

Donselaar, M.E., Overeem, I., 2008. Connectivity of fluvial point bar deposits: an example from the Miocene Huesca Fluvial Fan, Ebro Basin, Spain. AAPG Bull. 92, 1109–1129. https://doi.org/10.1306/04180807079.

Donselaar, M.E., Bhatt, A.G., Ghosh, A.K., 2017. On the relation between fluvio-deltaic flood basin geomorphology and the wide-spread occurrence of arsenic pollution in shallow aquifers. Sci. Total Environ. 574, 901–913. https://doi.org/10.1016/j.scitotenv.2016.09.074.

Douglas, G.M., Maffei, V.J., Zaneveld, J.R., et al., 2020. PICRUSt2 for prediction of metagenome functions. Nat. Biotechnol. 38, 685–688. https://doi.org/10.1038/s41587-020-0548-6.

Friend, P.F., Galloway, W.E., Hobday, D.K., 1996. Terrigenous Clastic Depositional Systems. Applications to Fossil Fuel and Groundwater Resources. Springer-Verlag, Berlin, Heidelberg, London, Paris, New York, Tokyo, Hong Kong xvi + 489 pp.

Ghosh, D., 2016. Distribution and biogeochemical cycling of arsenic. PhD ThesisLinköping Studies in Arts and Science. 670. Linköping University, Sweden 173 p.

Ghosh, D., Bhadury, P., 2018. Microbial cycling of arsenic in the aquifers of Bengal Delta Plains (BDP). In: Adhya, T.K., Lal, B., Mohapatra, B., Paul, D., Das, S. (Eds.), Advances in Soil Microbiology: Recent Trends and Future Prospects, 1st ed. Springer Singapore, pp. 91–108 https://doi.org/10.1007/978-981-10-6178-3_5.

Ghosh, D., Biswas, J.K., 2015. Biomonitoring macrophytes diversity and abundance for rating aquatic health of an oxbow lake ecosystem in Ganga River Basin. Am. J. Phytomed. Clin. Ther. 3, 602–621.

Ghosh, D., Routh, J., Bhadury, P., 2015a. Characterization and microbial utilization of dissolved lipid organic fraction in arsenic impacted aquifers (India). J. Hydrol. 527, 221–233. https://doi.org/10.1016/j.jhydrol.2015.04.051.

Ghosh, D., Routh, J., Dario, M., Bhadury, P., 2015b. Elemental and biomarker characteristics in a pleistocene aquifer vulnerable to arsenic contamination in the Bengal Delta Plain, India. Appl. Geochem. 61, 87–98. https://doi.org/10.1016/j.apgeochem.2015.05.007.

Ghosh, D., Bhadury, P., Routh, J., 2018. Coping with arsenic stress: adaptations of arsenite oxidizing bacterial membrane lipids to increasing arsenic levels. Microbiol. Open e594. https://doi.org/10.1002/mbo3.594.

Ghosh, A., Roy, M.B., Roy, P.K., 2020. Estimation and prediction of the oscillation pattern of meandering geometry in a sub-catchment basin of Bhagirathi-Hooghly river, West Bengal, India. SN Appl.Sci. 2, 1–24. https://doi.org/10.1007/s42452-020-03275-z.

Ghosh, D., Kumar, S., Donselaar, M.E., Corroto, C., Ghosh, A.K., 2021. Organic carbon transport model of abandoned river channels - a motif for floodplain geomorphology influencing biogeochemical swaying of arsenic. Sci. Total Environ. 762, 144400. https://doi.org/10.1016/j.scitotenv.2020.144400.

Glodowska, M., Stopelli, E., Schneider, M., Lightfoot, A., Rathi, B., Straub, D., Patzner, M., Duyen, V.T., Members, AdvectAs Team, Berg, M., Kleindienst, S., Kappler, A., 2020. Role of in situ natural organic matter in mobilizing As during microbial reduction of FeIII-mineral-bearing aquifer sediments from Hanoi (Vietnam). Environ. Sci. Technol. https://doi.org/10.1021/acs.est.9b07183.

Göd, R., Zemann, J., 1999. Native arsenic - realgar mineralization in marbles from Saualpe, Carinthia, Austria. Mineral. Petrol. 70, 37–53.

Goodbred Jr., S.L., Kuehl, S.A., 2000a. Enormous Ganges-Brahmaputra sediment discharge during strengthened early Holocene monsoon. Geology 28, 1083–1086.

Goodbred Jr., S.L., Kuehl, S.A., 2000b. The significance of large sediment supply, active tectonism, and eustasy on margin sequence development: Late Quaternary stratigraphy and evolution of the Ganges-Brahmaputra delta. Sediment. Geol. 133, 227–248.

Guha Mazumder, D.N., 2003. Chronic arsenic toxicity: clinical features, epidemiology, and treatment: experience in West Bengal. J. Environ. Sci. Health A Tox.Hazard. Subst. Environ. Eng. 38, 141–163. https://doi.org/10.1081/ESE-120016886.

Guo, H.M., Yang, S.Z., Tang, X.H., Li, Y., Shen, Z.L., 2008. Groundwater geochemistry and its implications for arsenic mobilization in shallow aquifers of the Hetao basin,Inner Mongolia. Sci. Total Environ. 393, 131–144. https://doi.org/10.1016/j.scitotenv.2007.12.025.

Harvey, C.F., 2002. Groundwater flow in the Ganges Delta. Science 296 (5573), 1563. https://doi.org/10.1126/science.296.5573.1563a.

Hoque, B.A., Yamaura, S., Sakai, A., Khanam, S., Karim, M., Hoque, Y., Hossain, S., Islam, S., Hossain, O., 2006. Arsenic mitigation for water supply in Bangladesh: appropriate

technological and policy perspectives. Water Qual. Res. J. Can. 41, 226–234. https://doi.org/10.2166/wqrj.2006.026.

Hoque, M.A., Khan, A.A., Shamsuddha, M., Hossain, M.S., Islam, T., Chowdhury, S.H., 2009. Near surface lithology and spatial variation of arsenic in the shallow groundwater: Southeastern Bangladesh. Environ. Geol. 56, 1687–1695. https://doi.org/10.1007/s00254-008-1267-3.

Hoque, M.A., McArthur, J.M., Sikdar, P.K., 2014. Sources of low-arsenic groundwater in the Bengal Basin: investigating the influence of the last glacial maximum palaeosol using a 115-km traverse across Bangladesh. Hydrogeol. J. 22, 1535–1547. https://doi.org/10.1007/s10040-014-1139-8.

Horton, T.W., Becker, J.A., Craw, D., Koons, P.O., Chamberlain, C.P., 2001. Hydrothermal arsenic enrichment in an active mountain belt: Southern Alps, New Zealand. Chem. Geol. 177, 323–339.

Hossain, M., Rahman, S.N., Bhattacharya, P., Jacks, G., Saha, R., Rahman, M., 2015. Sustainability of arsenic mitigation interventions—an evaluation of different alternative safe drinking water options provided in matlab, an arsenic hot spot in Bangladesh. Front. Environ. Sci. 30. https://doi.org/10.3389/fenvs.2015.00030.

Hossain, M., Bhattacharya, P., Jacks, G., von Brömssen, M., Ahmed, K.M., Hasan, M.A., Frape, S.K., 2017. Sustainable arsenic mitigation—from field trials to implementation for control of arsenic in drinking water supplies in Bangladesh. Best Practice Guide on the Control of Arsenic in Drinking Water. Metals and Related Substances in Drinking Water Series. IWA Publishing, UK, pp. 99–116.

Howard, G., Ahmed, M.F., Shamsuddin, A.J., Mahmud, S.G., Deere, D., 2006. Risk assessment of arsenic mitigation options in Bangladesh. J. Health Popul. Nutr. 24, 346.

Huang, G., Sun, J., Ying, Z., Jing, J., Zhang, Y., Liu, J., 2011. Distribution of arsenic in sewage irrigation area of Pearl River Delta, China. J. Earth Sci. 22, 396–410. https://doi.org/10.1007/s12583-011-0192-7.

Islam, M.R., Salminen, R., Lahermo, P.W., 2000. Arsenic and other toxic elemental contamination of groundwater, surface water and soil in Bangladesh and its possible effects on human health. Environ. Geochem. Health 22, 33–53.

Jakariya, M., Von Bromssen, M., Jacks, G., Chowdhury, A.M.R., Ahmed, K.M., Bhattacharya, P., 2007. Searching for a sustainable arsenic mitigation strategy in Bangladesh: experience from two upazilas. Int. J. Environ. Pollut. 31. https://doi.org/10.1504/IJEP.2007.016506.

Kavil, S.P., Ghosh, D., Pašić, I., Routh, J., 2020. Temporal dynamics of arsenic uptake and distribution: food and water risks in the Bengal basin. Toxicol. Environ. Chem. https://doi.org/10.1080/02772248.2020.1767781.

Kazmierczak, J., Postma, D., Dang, T., Van Hoang, H., Larsen, F., Hass, A.E., Hoffmann, A.H., Fensholt, R., Pham, N.Q., Jakobsen, R., 2022. Groundwater arsenic content related to the sedimentology and stratigraphy of the Red River deltaVietnam. Sci. Total Environ. 814, 152641. https://doi.org/10.1016/j.scitotenv.2021.152641.

Kriaa, A., Bourgin, M., Mkaouar, H., Jablaoui, A., Akermi, N., Soussou, S., Maguin, E., Rhimi, M., 2019. Microbial reduction of cholesterol to coprostanol: an old concept and new insights. Catalysts 9 (2), 167. https://doi.org/10.3390/catal9020167.

Kumar, A., Ali, M., Niraj, P.K., Akhouri, V., Kumar, V., Parwez, A., Rahman, M.S., Jain, P., Panjwani, G., Rajra, A., Rani, R., Kumar, R., Kumar, D., Singh, S., Bishwapriya, A., Kumar, S., Singh, M., Ghosh, A.K., 2021. Arsenic Induced Breast Cancer Risk in Population of Bihar, India. Research Square https://doi.org/10.21203/rs.3.rs-608639/v1.

Kumar, S., Ghosh, D., Donselaar, M.E., Burgers, F., Ghosh, A.K., 2021a. Clay-plug sediment as the locus of arsenic pollution in Holocene alluvial-plain aquifers. Catena 202, 105255. https://doi.org/10.1016/j.catena.2021.105255.

Kumar, S., Kumar, V., Saini, R.K., Pant, N., Singh, R., Singh, A., Kumar, M., 2021. Floodplains landforms, clay deposition and irrigation return flow govern arsenic occurrence, prevalence and mobilization: a geochemical and isotopic study of the mid-Gangetic floodplains. Environ. Res. 201, 111516. https://doi.org/10.1016/j.envres.2021.111516.

Lasseter, T.J., Waggoner, J.R., Lake, L.W., 1986. Reservoir heterogeneities and their influence on ultimate recovery. In: Lake, L.W., Carroll Jr., H.B. (Eds.), Reservoir Characterization. Academic Press, Orlando, pp. 545–559.

Lawson, M., Polya, D.A., Boyce, A.J., Bryant, C., Mondal, D., Shantz, Ballentine, C.J., 2013. Pond-derived organic carbon driving changes in arsenic hazard found in Asian groundwaters. Environ. Sci. Technol. 47, 7085–7094. https://doi.org/10.1021/es400114q.

Liu, G., Fernandez, A., Cai, Y., 2011. Complexation of arsenite with humic acid in the presence of ferric iron. Environ. Sci. Technol. 45, 3210–3216. https://doi.org/10.1021/es102931p.

Mallick, S., 2013. Landform and Channel Characteristics of Jamuna River Basin, West Bengal. MSc. thesisBarrackpore Rastraguru Surendranath College, West Bengal State Univ 61 p.

McArthur, J.M., Nath, B., Banerjee, D.M., Purohit, R., Grassineau, N., 2011. Palaeosol control on groundwater flow and pollutant distribution: the example of arsenic. Environ. Sci. Technol. 45, 1376–1383. https://doi.org/10.1021/es1032376.

Miall, A.D., 2014. Fluvial Depositional Systems. 14. Springer International Publishing 316 pp.

Michael, H.A., Voss, C.I., 2008. Evaluation of the sustainability of deep groundwater as an arsenic-safe resource in the Bengal Basin. Proc. Natl. Acad. Sci. 105, 8531–8536. https://doi.org/10.1073/pnas.0710477105.

Mondal, D., Rahman, M.M., Suman, S., Sharma, P., Siddique, A.B., Rahman, M.A., Bari, A.S.M.F., Kumar, R., Bose, N., Singh, S.K., Ghosh, A., Polya, D.A., 2021. Arsenic exposure from food exceeds that from drinking water in endemic area of Bihar, India. Sci. Total Environ. 754 (2021), 142082. https://doi.org/10.1016/j.scitotenv.2020.142082.

Mukherjee, A., Fryar, A.E., Howell, P.D., 2007. Regional hydrostratigraphy and groundwater flow modeling in the arsenic-affected areas of the western Bengal basin, West Bengal, India. Hydrogeol. J. 15 (7), 1397–1418.

Mukherjee, P.K., Pal, T., Chattopadhyay, S., 2010. Role of geomorphic elements on distribution of arsenic in groundwater–a case study in parts of Murshidabad and Nadia districts, West Bengal. Indian J. Geosci. 64, 77–86.

Mukherjee, A., Verma, S., Gupta, S., Henke, K.R., Bhattacharya, P., 2014. Influence of tectonics, sedimentation and aqueous flow cycles on the origin of global groundwater arsenic: paradigms from three continents. J. Hydrol. 518, 284–299. https://doi.org/10.1016/j.jhydrol.2013.10.044.

Mukherjee, A., Gupta, S., Coomar, P., Fryar, A.E., Guillot, S., Verma, S., Bhattacharya, P., Bundschuh, J., Charlet, L., 2019. Plate tectonics influence on geogenic arsenic cycling: from primary sources to global groundwater enrichment. Sci. Total Environ. 683, 793–807. https://doi.org/10.1016/j.scitotenv.2019.04.255.

Muyzer, G., de Waal, E.C., Uitterlinden, A.G., 1993. Profiling of complex microbial populations by denaturing gradient gel electrophoresis analysis of polymerase chain reaction-amplified genes coding for 16S rRNA. Appl. Environ. Microbiol. Microbiol. 59, 695–700. https://doi.org/10.1128/aem.59.3.695-700.1993.

Nath, B., Mallik, S.B., Stuben, D., Chatterjee, S., Charlet, L., 2010. Electrical resistivity investigation of arsenic affected alluvial aquifers in West Bengal, India: usefulness in identifying the areas of low and high groundwater arsenic. Environ. Earth Sci. 60, 873–884. https://doi.org/10.1007/s12665-009-0224-0.

Nickson, R., McArthur, J., Burgess, W., Ahmed, K.M., Ravenscroft, P., Rahman, M., 1998. Arsenic poisoning of Bangladesh groundwater. Nature 395, 338. https://doi.org/10.1038/26387.

Nickson, R.T., McArthur, J.M., Ravenscroft, P., Burgess, W.B., Ahmed, K.Z., 2000. Mechanism of arsenic release to groundwater in Bangladesh and West Bengal. Appl. Geochem. 15, 403–413.

Oblinger, J.L., Koburger, J.A., 1975. Understanding and teaching the most probable number technique. J. Milk Food Technol. 38, 540–545. https://doi.org/10.4315/0022-2747-38.9.540.

Parquer, M., Yan, N., Colombera, L., Mountney, N.P., Collon, P., Caumon, G., 2020. Combined inverse and forward numerical modelling for reconstruction of channel evolution and facies distributions in fluvial meander-belt deposits. Mar. Pet. Geol. 117, 104409. https://doi.org/10.1016/j.marpetgeo.2020.104409.

Podgorski, J., Berg, M., 2020. Global threat of arsenic in groundwater. Science 368 (6493), 845–850. https://doi.org/10.1126/science.aba1510.

Postma, D., Larsen, F., Thai, N.T., Trang, P.T.K., Jakobsen, R., Nhan, P.Q., Long, T.V., Pham, H.V., Murray, A.S., 2012. Groundwater arsenic concentration in Vietnam controlled by sediment age. Nat. Geosci. 5, 656–661. https://doi.org/10.1038/NGEO1540.

Postma, D., Mai, N.T.H., Lan, V.M., Trang, P.T.K., Sø, H.U., Nhan, P.Q., Larsen, F., Viet, P.H., Jakobsen, R., 2016. Fate of arsenic during Red River water infiltration into aquifers beneath Hanoi,Vietnam. Environ. Sci. Technol. 51, 838–845. https://doi.org/10.1021/acs.est.6b05065.

Rahman, M.A., Rahman, A., Khan, M.Z.K., Renzaho, A.M.N., 2018. Human health risks and socio-economic perspectives of arsenic exposure in Bangladesh: a scoping review. Ecotoxicol. Environ. Saf. 150, 335–343. https://doi.org/10.1016/j.ecoenv.2017.12.032.

Raju, N.J., 2022. Arsenic in the geo-environment: a review of sources, geochemical processes, toxicity and removal technologies. Environ. Res. 203, 111782. https://doi.org/10.1016/j.envres.2021.111782.

Ramos, O.E., Rötting, T.S., French, M., Sracek, O., Bundschuh, J., Quintanilla, J., Bhattacharya, P., 2014. Geochemical processes controlling mobilization of arsenic and trace elements in shallow aquifers and surface waters in the Antequera and Poopó mining regions, Bolivian Altiplano. J. Hydrol. 518, 421–433. https://doi.org/10.1016/j.jhydrol.2014.08.019.

Ravenscroft, P., Brammer, H., Richards, K., 2009. Arsenic in Asia. In: Ravenscroft, P., Brammer, H., Richards, K. (Eds.), Arsenic Contamination: A Global Synthesis. Wiley-Blackwell, Oxford, UK, pp. 318–386.

Reichwaldt, E.S., Ho, W.Y., Zhou, W., Ghadouani, A., 2017. Sterols indicate water quality and wastewater treatment efficiency. Water Res. 108, 401–411. https://doi.org/10.1016/j.watres.2016.11.029.

Robinson, C., Von Brömssen, M., Bhattacharya, P., Häller, S., Bivén, A., Hossain, M., Thunvik, R., 2011. Dynamics of arsenic adsorption in the targeted arsenic-safe aquifers in Matlab, south-eastern Bangladesh: insight from experimental studies. Appl. Geochem. 26, 624–635. https://doi.org/10.1016/j.apgeochem.2011.01.019.

Roychowdhury, R., Khan, M.H., Choudhury, S., 2018. Arsenic in rice: an overview on stress implications, tolerance and mitigation strategies. In: Hasanuzzaman, M., Nahar, K., Fujita, M. (Eds.), Plants Under Metal and Metalloid Stress. Springer, Singapore https://doi.org/10.1007/978-981-13-2242-6_15.

Saha, K.C., 2003. Diagnosis of arsenicosis. J. Environ. Sci. Health A 38, 255–272. https://doi.org/10.1081/ESE-120016893.

Sahana, M., Rihan, M., Deb, S., Patel, P.P., Ahmad, W.S., Imdad, K., 2020. Detecting the facets of anthropogenic interventions on the palaeochannels of Saraswati and Jamuna. In: Das, B.C., Ghosh, S., Islam, A., Roy, S. (Eds.), Anthropogeomorphology of Bhagirathi-Hooghly River System in India. CRC Press/Taylor & Francis Group, Boca Raton, USA, pp. 469–490 https://doi.org/10.1201/9781003032373.

Sahu, S., Saha, D., 2015. Role of shallow alluvial stratigraphy and holocene geomorphology on groundwater arsenic contamination in the Middle Ganga Plain, India. Environ. Earth Sci. 73, 3523–3536. https://doi.org/10.1007/s12665-014-3637-3.

Sathe, S.S., Mahanta, C., 2019. Groundwater flow and arsenic contamination transport modeling for a multi aquifer terrain: assessment and mitigation strategies. J. Environ. Manag. 231, 166–181. https://doi.org/10.1016/j.jenvman.2018.08.057.

Seddique, A.A., Masuda, H., Mitamura, M., Shinoda, K., Yamanaka, T., Itai, T., Maruoka, T., Uesugi, K., Ahmed, K.M., Biswas, D.K., 2008. Arsenic release from biotite into a Holocene groundwater aquifer in Bangladesh. Appl. Geochem. 23, 2236–2248. https://doi.org/10.1016/j.apgeochem.2008.03.007.

Sharma, P., Ofner, J., Kappler, A., 2010. Formation of binary and ternary colloids and dissolved complexes of organic matter, Fe and As. Environ. Sci. Technol. 44, 4479–4485. https://doi.org/10.1021/es100066s.

Sikdar, P.K., Chakraborty, S., 2017. Numerical modelling of groundwater flow to understand the impacts of pumping on arsenic migration in the aquifer of North Bengal Plain. J.Earth Syst.Sci. 126 (2), 1–22. https://doi.org/10.1007/s12040-017-0799-x.

Singh, A., Patel, A.K., Kumar, M., 2022. Impact of river fluvial processes on arsenic enrichment in Mid Gangetic Plains: the coining of arsenic confirming pollution markers. Environ. Res. 203, 111741. https://doi.org/10.1016/j.envres.2021.111741.

Smedley, P.L., Kinniburgh, D.G., 2002. A review of the source, behavior and distribution of arsenic in natural waters. Appl. Geochem. 17, 517–568.

Stecher, G., Tamura, K., Kumar, S., 2020. Molecular evolutionary genetics analysis (MEGA) for macOS. Mol. Biol. Evol. 37, 1237–1239. https://doi.org/10.1093/molbev/msz312.

Stopelli, E., Duyen, V.T., Mai, T.T., Trang, P.T.K., et al., 2020. Spatial and temporal evolution of groundwater arsenic contamination in the Red River delta, Vietnam: interplay of mobilisation and retardation processes. Sci. Total Environ. 717, 137143. https://doi.org/10.1016/j.scitotenv.2020.137143.

Tapia, J., Murray, J., Ormachea, M., Tirado, N., Nordstrom, D.K., 2019. Origin, distribution, and geochemistry of arsenic in the Altiplano-Puna plateau of Argentina, Bolivia, Chile, and Perú. Sci. Total Environ. 678, 309–325. https://doi.org/10.1016/j.scitotenv.2019.04.084.

Trung, D.T., Nhan, N.T., Don, T.V., Hung, N.K., Kazmierczak, J., Nhan, P.Q., 2020. The controlling of paleo-riverbed migration on arsenic mobilization in groundwater in the red River DeltaVietnam. Vietnam J. Earth Sci. 42, 161–175. https://doi.org/10.15625/0866-7187/42/2/14998.

Van Geen, A., Zheng, Y., Goodbred Jr., S., Horneman, A., Aziz, Z., Cheng, Z., et al., 2008. Flushing history as a hydrogeological control on the regional distribution of arsenic in shallow groundwater of the Bengal Basin. Environ. Sci. Technol. 42, 2283–2288. https://doi.org/10.1021/es702316k.

Van Geen, A., Bostick, B.C., Thi Kim Trang, P., Lan, V.M., Mai, N.N., Manh, P.D., Berg, M., 2013. Retardation of arsenic transport through a Pleistocene aquifer. Nature 501 (7466), 204–207. https://doi.org/10.1038/nature12444.

Wallis, I., Prommer, H., Berg, M., Siade, A.J., Sun, J., Kipfer, R., 2020. The river–groundwater interface as a hotspot for arsenic release. Nat. Geosci. 13, 288–295. https://doi.org/10.1038/s41561-020-0557-6.

Weinman, B., Goodbred, S.L., Zheng, Y., Aziz, Z., Steckler, M., van Geen, A., et al., 2008. Contributions of floodplain stratigraphy and evolution to the spatial patterns of groundwater arsenic in Araihazar, Bangladesh. Geol. Soc. Am. Bull. 120, 1567–1580. https://doi.org/10.1130/B26209.1.

World Health Organization (WHO), 2011. Guidelines for Drinking-Water Quality. 4th ed. Geneva, 541 p.

Wu, W., Ruan, J., Ding, S., Zhao, L., Xu, Y., Yang, H., Ding, W., Pei, Y., 2014. Source and distribution of glycerol dialkyl glycerol tetraethers along lower Yellow River estuary–coast transect. Mar. Chem. 158, 17–26. https://doi.org/10.1016/j.marchem.2013.11.006.

Wu, X., Bowers, B., Kim, D., Lee, B., Jun, Y.S., 2019. Dissolved organic matter affects arsenic mobility and iron(III) (hydr)oxide formation: implications for managed aquifer recharge. Environ. Sci. Technol. 53 (24), 14357–14367. https://doi.org/10.1021/acs.est.9b04873.

Zhao, F.J., Wang, P., 2020. Arsenic and cadmium accumulation in rice and mitigation strategies. Plant Soil 446, 1–21.

Zhao, F.-J., McGrath, S.P., Meharg, A.A., 2010. Arsenic as a food chain contaminant: mechanisms of plant uptake and metabolism and mitigation strategies. Annu. Rev. Plant Biol. 61, 535–559. https://doi.org/10.1146/annurev-arplant-042809-112152.